35th Annual International Conference of the IEEE EMBS
Osaka, Japan, 3 - 7 July, 2013

Active Control of Microbubbles Stream in Multi-bifurcated Flow by Using 2D Phased Array Ultrasound Transducer*

Ren Koda, Jun Koido, Naoto Hosaka, Takumi Ito, Shinya Onogi, Takashi Mochizuki, Kohji Masuda, *Member, IEEE*, Seiichi Ikeda, Fumihito Arai, *Member, IEEE*

***Abstract*— We have previously reported our attempt to propel microbbles in flow by a primary Bjerknes force, which is a physical phenomenon where an acoustic wave pushes an obstacle along its direction of propagation. However, when ultrasound was emitted from surface of the body, controlling bubbles in against flow was needed. It is unpractical to use multiple transducers to produce the same number of focal points because single element transducer cannot produce more than two focal points. In this study, we introduced a complex artificial blood vessel according to a capillary model and a 2D array transducer to produce multiple focal points for active control of microbubbles in against flow. Furthermore, we investigated bubble control in viscous fluid. As the results, we confirmed clearly path selection of MBs in viscous fluid as well as in water.**

I. Introduction

Because the oscillation of microbubbles (MBs) under continuous ultrasound exposure accelerates the temperature increase at a focal area, MBs are utilized for ultrasound thermal therapy [1] to improve the efficiency of high intensity focused ultrasound (HIFU) therapy. Also, because the existence of bubbles induces sonoporation [2] upon ultrasound exposure, MBs are utilized for physical drug delivery [3] to allow the uptake of larger molecules into cells. The advantage of these therapies is the ease in determining the distribution of MBs inside the body through the variation of brightness on echograms. However, it is difficult to prevent bubbles from passing through the desired target area due to the diffusion of bubbles after injection into the human body. If the behavior of bubbles could be controlled to enhance the local concentration of bubbles, not only the side effects would be minimized but also the efficiency of the treatment would be increased.

We have ever reported our attempts to control MBs using the primary and secondary acoustic force to elucidate the conditions in sound pressure, central frequency of ultrasound, and flow velocity for active path selection of MBs in water flow using artificial blood vessels with a simple shape [4]. However, the system construction of arteries was outward branch. When ultrasound was emitted from surface of the body, controlling bubbles in against flow was needed. In our previous research, the direction of ultrasound propagation was in forward to the flow and the bubbles were propelled along the direction of propagation of ultrasound. Furthermore, blood viscosity is one of the important factors determining the behavior of MBs in flow. *In vivo* conditions, the ideal bubble control might not to be ensured due to the limitation of emit angle of ultrasound and the blood viscosity. And more, it is unpractical to use multiple transducers to produce the same number of focal points because single element transducer cannot produce more than two focal points.

To solve these problems, we have investigated acoustic forces along the gradient of sound pressure. Fig.1 shows the conceptual rendering. With multiple focal points formation around the bifurcations, an ideal bubble control should be realized. The purposes of this study were to control of MBs in against flow by producing multiple focal points for reduction of sound sources and to realize bubble control in viscous fluid. In this study, we investigated the position of focal point to control MBs in against flow and compared the controllability of MBs in the fluid condition of water and viscous medium.

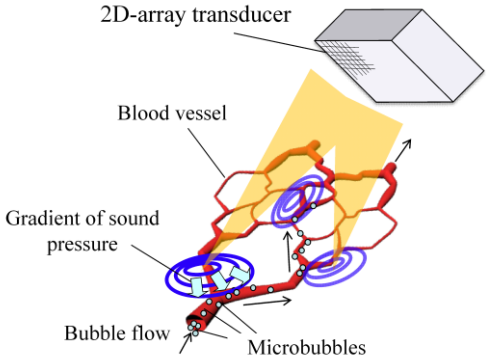

Figure 1. Bubble control by acoustic forces along with the gradient of sound pressure.

II. Experiments

A. Artificial blood vessel and viscous fluid

We have prepared an artificial blood vessel according to the capillary model which was made of the mixture material of wax and poly(vinyl alcohol) (PVA) [5]. The inflow path of 2 mm was repeatedly divided into two lower courses to constitute the artificial capillary until the middle of the model, where the minimum path width was 0.50 mm. The path widths and the section areas are designed to guarantee a constant flow velocity in any part of the model.

We have also prepared a Doppler test fluid (707 model, ATS lab.) as a viscous fluid. The fluid is a dispersion of plastic

* This research is granted by the Japan Society for the Promotion of Science (JSPS) through the Funding Program for Next Generation World-Leading Researchers (NEXT Program).

Ren Koda, Jun Koido, Naoto Hosaka, Takumi Ito, Shinya Onogi, Takashi Mochizuki and Kohji Masuda are with Graduate School of Bio-Applications and Systems Engineering, Tokyo University of Agriculture and Technology, Koganei, Tokyo, 184-8588 Japan (e-mail: 50011701301@st.tuat.ac.jp).

Seiichi Ikeda, Fumihito Arai are with Nagoya University, Nagoya, 466-8550 Japan

particles as quasi blood cells in a glycerin water mixture. The sound velocity (1570 m/s), density (1.0 g/mL) and viscosity (1.66 centistorkes) are similar to that of blood plasma, though the particle concentration (< 1 %) and the diameter (30 μm) are not similar to that of blood cells.

B. *Sound sources*

We have prepared two types of sound sources, which were a single disc transducer including a plane ceramic disc and a 2D matrix array transducer. One of the transducers, a single disc transducer (T_{ag}) was to produce MBs aggregations at the upper stream of the paths. The central frequency of T_{ag} was set in 7 MHz which was close to resonance frequency of MB, according to our previous paper [6]. The other, 2D array matrix transducer (T_{in}) was to propel the MB aggregates and induce to a desired path. T_{in} has air-backed 64 PZT elements with the aperture of 23.9 x 23.9 mm^2, the size of each element of 2.9 x 2.9 mm^2, and the pitch of the elements of 3.0 mm, respectively. The central frequency of the element is 1 MHz, where the drive unit was required to produce continuous square wave with minimum delay pitch of 5 ns.

Settings of delay times in each element were calculated as following procedures: When we assume the medium is water, we have obtained absolute arrival times of the ultrasound by dividing a distance between the focal point and the each element by sound speed of the medium. We have also obtained relative delay times on each element by subtraction the each arrival times from the maximum. We set the farthest element as a benchmark and the element was initially driven. The other elements are driven according to relative delay time. Then, the focal point could be formed.

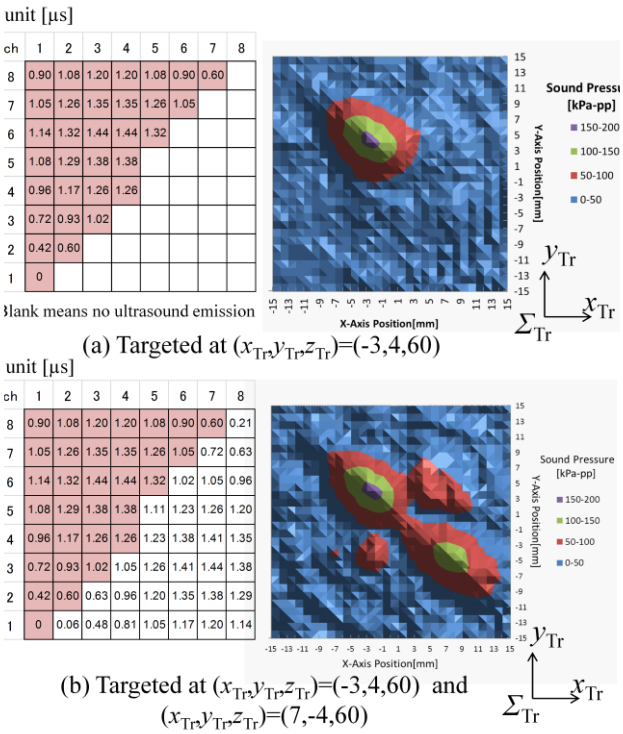

Figure 2. Map of delay pitches (left) and sound pressure distribution (right) of 32 and 64 elements.

We calculated delay time of divided in two parts with 32 elements. Fig.2 (left) shows the distribution of delay times which were calculated to produce single focal point and multiple focal points. One is a single focal point pattern of $(x_{Tr},y_{Tr},z_{Tr})=(-3,4,60)$ by the 32 elements. The other is additional focal point pattern of $(x_{Tr},y_{Tr},z_{Tr})=(7,-4,60)$ by the other 32 elements. Their quantized delay pitch was 30 ns. The blanks mean no ultrasound emission. Fig.2 (right), shows sound pressure distributions which were measured by a hydrophone (ONDA, HNR1000) in the distance of 60 mm from the surface of 2D array transducer in degased water.

C. *Experimental setup*

We used the F-04E microbubble [4,6], which has a shell made of poly (vinyl chloride) and an average diameter of 4 μm. Artificial blood vessel discussed in the above section was fixedly floated 30 mm from the bottom of a water tank, which is filled with water, to guarantee the working distance of an optical microscope (Omron KH-7700, 15 fps) to observe the path through the transparent bottom plate of the tank. Fig. 3 shows the outlook of the experimental setup. The paths width correspond to 1.4, 1.0, 0.7 mm. P1 to P9 and Q1 to Q9 mean focal points by T_{in} which are controlled 2 mm pitch in Tr coordination, though the pitch was 3.1 mm in x direction of the capillary coordination due to an elevation angle of T_{in}. We set the focal point of T_{ag} to correspond to the center of the axis of the artificial blood vessel at 10 mm upper stream from the first bifurcation. The angle of the axis of the transducers were set at θ_{ag}= 60° and θ_{in}= 40° to avoid physical interference of both the source of light and the edge of the tank. The distance from the artificial blood vessel of both transducers were set at $d_{ag} = d_{in}$ = 60 mm. The suspension of MBs was prepared at a concentration of 1.18 μL/ml. A 5 mL aliquot of the suspension was sampled and injected into the flow using a syringe. The duration of injection of the suspension was controlled by a rotary pump to finish 30 s after the beginning of the injection with the flow speed of 40 mm/s.

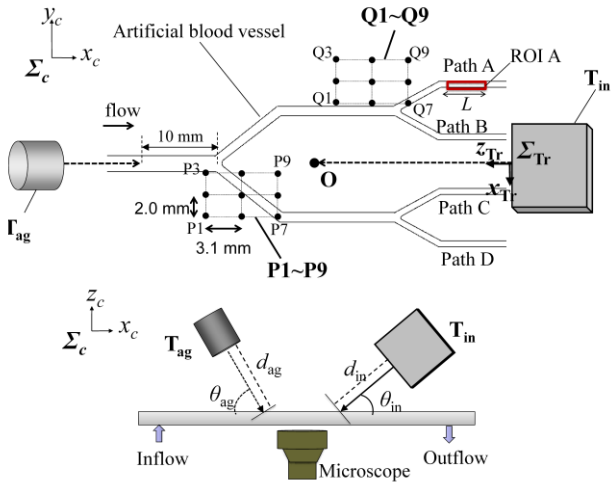

Figure 3. Schematic of the experiment with the artificial blood vessel of capillary model and the ultrasound transducers.

D. *Evaluation of the amount of microbubbles through each path*

To measure the amount of MBs, we established four square regions of interest (ROI A, B, C and D) in each path (Path A, B, C and D). ROI A is shown in Fig.3. The width of ROI was corresponding with the path width and the length of ROI (L) was calculated by dividing a flow speed by flame rate. Then, the size of ROI is 0.7 x 2.6 mm^2 (16 x 58 pixels). We calculated the average brightness. In our previous paper [4], we evaluated the amount of bubbles by defining the induction index, which reflects the brightness according to the existence of bubbles in two paths. However, the value of the induction index cannot be compared between four ROIs. Thus, we have defined the rate of bubbles amount ξ_A, ξ_B, ξ_C and ξ_D. For example ξ_A, the proportion of bubbles passed Path A, was calculated using the following equation:

$$\xi_A = \frac{\sigma_A}{\sigma_A + \sigma_B + \sigma_C + \sigma_D} \times 100 \quad [\%] \tag{1}$$

$$\sigma_A = (I_{A0} - I_A) \times \alpha \tag{2}$$

where I_{A0} indicate initial brightness average without bubbles, and I_A indicate brightness average with bubbles, in the ROI A. α is an expediential coefficient for the sake of argument. We have confirmed a liner relationship between bubble concentration and σ in the preliminary experiment with the range of bubble concentration as following experiment.

III. Results

We verified the position of the focal point from T_{in}, where P1 to P9 near the first bifurcation. Figs.4 (i)-(ii) show the microscopic images of the bifurcations upon ultrasound emission from T_{in} was focused on P6 and P5, respectively. The distributions of sound pressure in the observation area were calculated using the Rayleigh equation and superimposed on the microscope image over 50 kPa-pp. Here the distribution of sound pressure was obtained as follows; the sound pressure of the focal point was directly measured by using a hydrophone to derive magnitude of sound pressure and the value was relatively converted to the normalized distribution. The maximum sound pressure was about 150 kPa-pp. In Fig.4 (i),

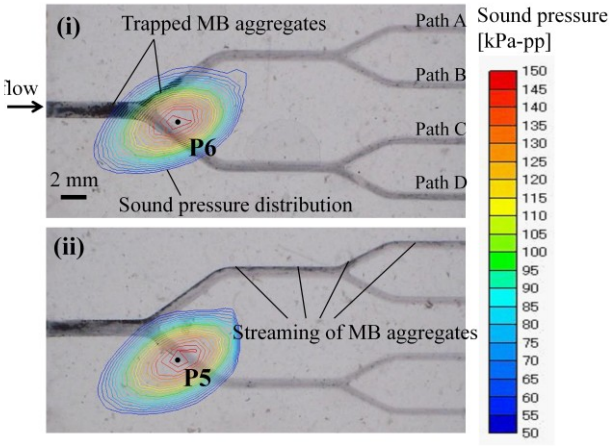

Figure 4. Microscopic results with the distribution of sound pressure targeted at the first bifurcation.

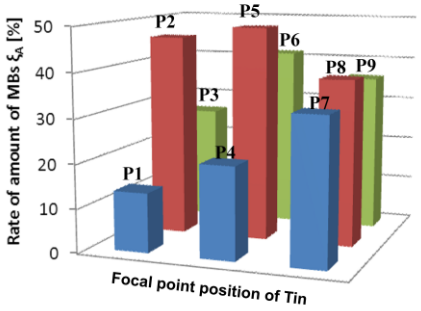

Figure 5. Rate of amount of MBs (ξ_A) vs. focal point position targeted at the first bifurcation.

bigger aggregations of MBs were confirmed with a focal point at P6 which position near the first bifurcation. In Fig.4 (ii), when a focal point at P5, the streaming of MBs was smoothly propelled to Path A.

Fig. 5 shows the rate of amount of MBs through Path A (ξ_A) vs. focal point position from T_{in} around the first bifurcation. In case the focal point was positioned at P2 or P5, the rate of amount of MBs in Path A was higher. Then, we fixed the focal point position toward the first bifurcation at P5 in followed experiments.

Next, we examined the same procedure, toward the second bifurcation where the multiple focal points were positioned. One of the focal points was fixed at P5. The other was positioned in Q1 to Q9. Figs.6 (i)-(ii) show the microscope images of the observation area overlapped sound pressure distribution of Q5 and Q4. In Fig.6 (i), when the emission was at Q5, the streaming of MBs was smoothly flown to Path B. In Fig.6 (ii), at the focal point of Q4, most of MBs were trapped on the second bifurcation.

Fig. 7 shows the rate of amount of MBs through Path B (ξ_B) vs. exposure position from T_{in} around the second bifurcation. In this experiment we found that about 40 % of MB passed to Path B with the focal points located P5 and Q5.

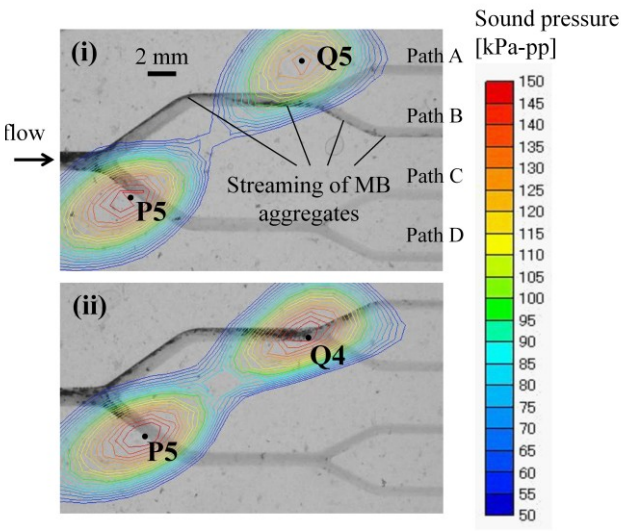

Figure 6. Microscopic results with the distribution of sound pressure targeted at the first bifurcation and the second bifurcation.

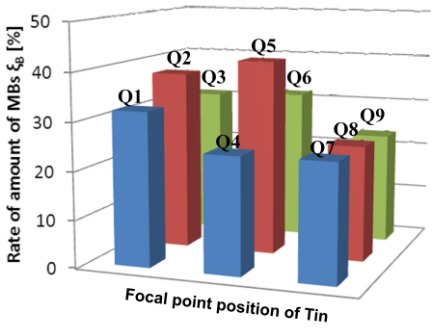

Figure 7. Rate of amount of MBs (ξ_B) vs. focal point position targeted the second bifurcation

We have compared the effect of the fluid by changing the fluid condition in water or viscous fluid. From the results in Figs.5 and 7, we selected the parameters of focal points positions of T_{in} as P5 and Q5. Fig.8 shows the microscopic images of the bifurcation upon emission of sinusoidal ultrasound of T_{ag} and T_{in} in viscous fluid. In Fig.8 (i) when ultrasound was emitted to P5 from T_{in}, clearly path selection to Path A was confirmed. In Fig.8 (ii), switched pattern of acoustic field to P5 and Q5, the streaming of aggregates entered to Path B. Fig. 9 shows the rate of amount of MBs vs. condition of exposure pattern and fluid. The standard deviation of three trials was also shown in the figure. In this experiment, the viscosity dependence of fluid was not confirmed. We have to investigate the behavior of MBs more precisely under various viscosities of fluid. From these results, we confirmed clearly path selection of MBs in viscous fluid as well as in water.

In the next step, we are going to elucidate the behavior of bubbles in the fluid condition of the human blood before applying it to an *in vivo* experiment. The effects of hematocrit and blood pressure of human blood should be considered by analyzing the bubble behavior by numerical simulation. Meanwhile, we are going to develop a method to identify the precise location of bifurcations *in vivo* by detecting and constructing the three-dimensional shape of the blood vessel.

IV. Conclusion

In this study, we investigated the position of focal point and the fluid condition to control bubble in against flow by acoustic forces along the gradient of sound pressure. First, the optimum position of focal point around the first and the second bifurcations was investigated. With multiple focal points formation at multi-bifurcations, we showed the probably of reduction sound sources. Path selection of MBs to Path A and B was realized without change position and pose of 2D array transducer. Second, bubble control in viscous fluid was investigated. We showed the bubble control in viscous fluid was successfully realized as well as in water. We are going to continue our research by varying other parameters in this experiment before conducting an *in vivo* experiment.

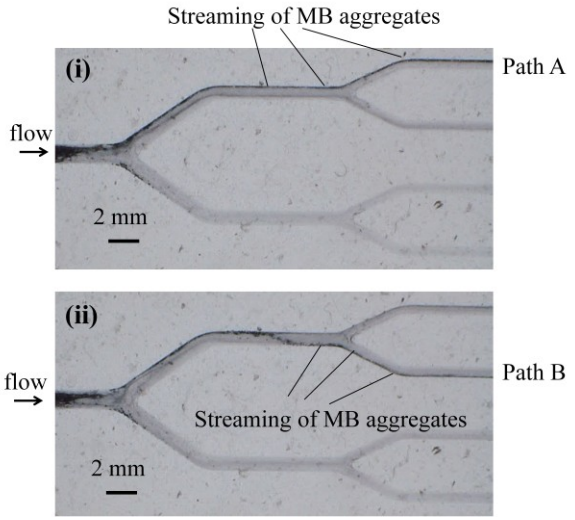

Figure 8. Microscopic results with the sound pressure targeted at the first bifurcation (i) and both the first and second bifurcation (ii) in viscous fluid.

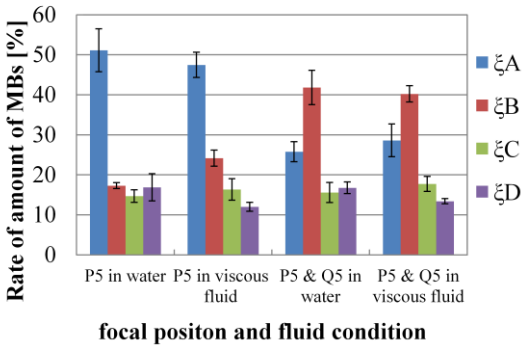

Figure 9. Rate of amount of MBs vs. condition of exposure pattern and fluid.

References

[1] CH Farny, RG Holt and RA Roy, "The Correlation Between Bubble-Enhanced HIFU Heating and Cavitation Power", Biomedical Engineering, *IEEE Trans. Biomedical Engineering*, vol. 57, No. 1, January 2010

[2] K. Osawa, Y. Okubo, K. Nakao, N. Koyama, and K. Bessho: "Osteoinduction by microbubble-enhanced transcutaneous sonoporation of human bone morphogenetic protein-2," *J. Gene Med.* vol.11, No.7, pp.633-41, 2009.

[3] L. J. M. Juffermans, A. van Dijk, C. A. M. Jongenelen, B. Drukarch, A. Reijerkerk, H. E. de Vries, O. Kamp, and R. J. P. Musters: "Ultrasound and Microbubble-Induced Intra- and Intercellular Bioeffects in Primary Endothelial Cells ," *Ultrason. Med. Biol.* Vol.35, No.11, pp.1917-1927, 2009.

[4] K. Masuda, N. Watarai, R. Nakamoto, et al, "Production of local acoustic radiation force to constrain direction of microcapsules in flow," *Jap. J. Applied Physics*, Vol.49, 07HF11, 2010.

[5] K. Masuda, N. Shigehara, R. Koda, N. Watarai, S. Ikeda, F. Arai, Y. Miyamoto and T. Chiba: "Observation of Flow Variation in Capillaries of Artificial Blood Vessel by Producing Microbubble Aggregations," *Proc. of 34th Annual Int'l Conf. EMBS*, 2064-2067, 2012

[6] R. Koda, N. Watarai, R. Nakamoto, T. Ohta, K. Masuda, Y. Miyamoto and T. Chiba: " Dependence of Aggregate Formation of Microbubbles upon Ultrasound Condition and Exposure Time," *Proc. of 33rd Annual Int'l Conf. EMBS*, 5589-5592, 2011